Int. J. Appl. Math. Comput. Sci., , Vol. , No. , –
DOI:

amcs

NUMERICAL SOLUTIONS TO INTEGRAL EQUATIONS EQUIVALENT TO DIFFERENTIAL EQUATIONS WITH FRACTIONAL TIME

BARTOSZ BANDROWSKI *, ANNA KARCZEWSKA *, PIOTR ROZMEJ **

* Faculty of Mathematics, Computer Science and Econometrics, University of Zielona Góra
ul. Szafrana 4a, 65-516 Zielona Góra, Poland
email: {B.Bandrowski, A.Karczewska}@wmie.uz.zgora.pl

** Institute of Physics, University of Zielona Góra
ul. Szafrana 4a, 65-516 Zielona Góra, Poland
email: P.Rozmej@if.uz.zgora.pl

This paper presents an approximate method of solving the fractional (in time variable) equation which describes the processes lying between heat and wave behavior. The approximation consists in application of finite subspace of the infinite basis in time variable (Galerkin method) and discretization in space variables. In the final step a huge system of linear equations with non-symmetric matrix is solved with the use of iterative (GMRES) method.

Keywords: Fractional equations, Galerkin method, anomalous diffusion.

1. Introduction

Several physical phenomena show anomalous transport properties. Generally diffusive properties are classified as normal if their variance grows linearly in time and as anomalous if the variance growth is different than the linear one. In recent years there is an increasing interest in dynamical processes occuring in systems exhibiting anomalous diffusive behavior. Such systems range from physics and chemistry to biology and medicine (Meltzer and Klafter, 2000). Dispersion in complex plasmas (Ratynskaia *et al*., 2006), self-diffusion of surfactant molecules (Gambin *et al*., 2005), light in cold atomic cloud (Labeyrie *et al*., 2003) and donor-acceptor electron pairs within a protein (Kou and Sunney Xie, 2004) are examples of the more recent experimental evidences. Several papers (Goychuk *et al*., 2006; Heinsalu *et al*., 2006; Heinsalu *et al*., 2009) consider fractional Fokker-Planck equation both in analytical and numerical approach. Fractional time approach is considered also in the theory of control, see e.g. (Kaczorek, 2008; Guermah *et al*., 2008). An interesting numerical approach to partial differential equation of fractional order in space variable has been presented by (Ciesielski and Leszczyński, 2006).

In most of numerical applications to fractional differential or fractional integro-differential equations the application of numerical methods is limited to 1+1 (time+space) dimensions. Our paper presents a different method for solving fractional integro-differential equation which can handle more dimensional cases within a good approximation. The method is limited to cases when the initial condition $u(x,0)$ is smooth enough with respect to space variables x. In such cases it works also for (1+2) and (1+3) dimensions.

We consider the following Volterra equation

$$u(x,t) = u(x,0) + \int_0^t a(t-s)\Delta u(x,s)ds, \qquad (1)$$

where $x \in \mathbb{R}^d$, $t > 0$, $a(t) = \frac{t^{\alpha-1}}{\Gamma(\alpha)}$, Γ is the gamma function, $\alpha \in [1,2]$ and Δ is the Laplace operator.

Because of the form of the kernel function a, the integral in equation (1) is a Riemann-Liouville fractional integral operator (Bazhlekova, 2001)

$$J_t^\alpha f(t) := \int_0^t \frac{1}{\Gamma(\alpha)}(t-s)^{\alpha-1} f(s)ds.$$

Applying the Caputo fractional derivative operator to (1) one obtains a fractional differential equation

$$\frac{\partial^\alpha}{\partial t^\alpha} u(x,t) = \Delta u(x,t), \qquad (2)$$

where $\alpha \in [1,2]$, $x \in \mathbb{R}^d$, $t > 0$ and Δ is the Laplace operator.

For particular cases $\alpha = 1$ and $\alpha = 2$, taking appropriate initial conditions, the equation (2) is the heat and the wave equation, respectively. For $\alpha \in (1,2)$ the equation (2) interpolates the heat and the wave equations.

The equation (1) was discussed by Fujita (Fujita, 1990) and Schneider and Wyss (Schneider and Wyss, 1989). Fujita has found the analytical solution $u(x,t)$ to (1) in terms of fundamental solutions using Mittag-Leffler functions. Schneider and Wyss applied Green function method and obtained the analytical form of solution in terms of Wright functions (which are related to Mittag-Leffler functions). Both approaches are limited to 1+1-dimensional case and practically non-computable.

2. Construction of numerical solution

The numerical approach described below follows in general that described in (Rozmej and Karczewska, 2005).

Let be given a set of real orthonormal functions $\{\phi_j : j = 1,2,...,\infty\}$ on the interval $[0,t]$, spanning a Hilbert space H with an inner product

$$\langle f,g\rangle := \int_0^t f(\tau)g(\tau)W(\tau)d\tau,$$

where W is a weight function.

An approximate solution to (1) is considered as an element of the subspace H_n spanned by n first basis functions $\{\phi_k : k = 1,2,...,n\}$

$$u_n(x,t) = \sum_{k=1}^{n} c_k(x)\phi_k(t). \tag{3}$$

Inserting (3) into (1) one obtains

$$u_n(x,t) = u(x,0) + \int_0^t a(t-s)\Delta u_n(x,s)ds + \epsilon_n(x,t), \tag{4}$$

where ϵ_n denotes the approximation error. From (3) and (4) we get the form of the error function

$$\begin{aligned}\epsilon_n(x,t) &= \sum_{k=1}^{n} c_k(x)\phi_k(t) - u(x,0) \\ &- \int_0^t a(t-s)\sum_{k=1}^{n}\frac{d^2}{dx^2}c_k(x)\phi_k(s)ds. \end{aligned}\tag{5}$$

Definition 1. Galerkin approximation of the solution to equation (1) is a function $u_n \in H_n$ such that $\epsilon_n \perp H_n$, i.e.

$$\forall_{k=1,2,...,n} \quad \langle \epsilon_n(x,t), \phi_k(t)\rangle = 0.$$

From Definition 1 and (5) we obtain

$$\begin{aligned} 0 = &\int_0^t \left[\sum_{k=1}^{n} c_k(x)\phi_k(\tau)\right]\phi_j(\tau)W(\tau)d\tau - \\ &\int_0^t u(x,0)\phi_j(\tau)W(\tau)d\tau - \\ &\int_0^t \left[\int_0^\tau a(\tau-s)\sum_{k=1}^{n}\frac{d^2}{dx^2}c_k(x)\phi_k(s)ds\right]\phi_j(\tau)W(\tau)d\tau. \end{aligned}$$

for $j = 1,2,...,n$, which means that

$$\begin{aligned} &\int_0^t u(x,0)\phi_j(\tau)W(\tau)d\tau = \\ &\int_0^t \left[\sum_{k=1}^{n} c_k(x)\phi_k(\tau)\right]\phi_j(\tau)W(\tau)d\tau - \\ &\int_0^t \left[\int_0^\tau a(\tau-s)\sum_{k=1}^{n}\frac{d^2}{dx^2}c_k(x)\phi_k(s)ds\right]\phi_j(\tau)W(\tau)d\tau. \end{aligned}$$

The above equations may be written in shortened form

$$g_j(x) = c_j(x) - \sum_{k=1}^{n} a_{jk}\frac{d^2}{dx^2}c_k(x), \tag{6}$$

where

$$a_{jk} = \int_0^t \left[\int_0^\tau a(\tau-s)\phi_k(s)ds\right]\phi_j(\tau)W(\tau)d\tau$$

and

$$g_j(x) = u(x,0)\int_0^t \phi_j(\tau)W(\tau)d\tau,$$

$j = 1,2,...,n$. In general $a_{jk} \neq a_{kj}$.

Equations (6) describe the set of coupled differential equations for the coefficient functions $c_k(x)$, $k = 1,2,...,n$ determining approximate solution (3).

To solve the set (6) we use standard, centered three-point finite difference approximation to the second derivative (Laplacian).

In one spatial dimension one obtains (6) as

$$\begin{aligned} g_j(x_i) &= c_j(x_i) \\ &+ \frac{1}{h^2}\sum_{k=1}^{n} a_{jk}\left[-c_k(x_{i-1}) + 2c_k(x_i) - c_k(x_{i+1})\right], \end{aligned}\tag{7}$$

where $x_i - x_{i-1} = h$ and $j = 1,2,...,n$, $i = 1,2,...,m$. For two spatial dimensions, and homogenous grid, (6) can

be written as

$$\begin{aligned} g_j(x_i,y_l) &= c_j(x_i,y_l) \\ &+ \frac{1}{h^2}\sum_{k=1}^{n} a_{jk}[-c_k(x_{i-1},y_l)-c_k(x_i,y_{l-1}) \\ &+ 4c_k(x_i,y_l)-c_k(x_{i+1},y_l)-c_k(x_i,y_{l+1})], \end{aligned} \tag{8}$$

where $x_i - x_{i-1} = y_l - y_{l-1} = h$ and $j = 1, 2, ..., n$, $i = 1, 2, ..., m$, $l = 1, 2, ..., m$.

The sets (7) and (8) can be presented in the matrix form

$$g = \mathcal{A}c, \tag{9}$$

where the vectors g, c and the matrix $\mathcal{A}$ have a block structure

$$g=\begin{pmatrix} G_1 \\ G_2 \\ \vdots \\ G_n \end{pmatrix},\ c=\begin{pmatrix} C_1 \\ C_2 \\ \vdots \\ C_n \end{pmatrix},\ \mathcal{A}=\begin{pmatrix} [A_{11}] & \cdots & [A_{1n}] \\ [A_{21}] & \cdots & [A_{2n}] \\ \vdots & \ddots & \vdots \\ [A_{n1}] & \cdots & [A_{nn}] \end{pmatrix}. \tag{10}$$

In one-dimensional case (7) we have for (10)

$$G_j^T = (g_j(x_1), g_j(x_2), \ldots, g_j(x_m))$$

and

$$C_j^T = (c_j(x_1), c_j(x_2), \ldots, c_j(x_m)),$$

where G_j^T and C_j^T stand for transpose of vectors G_j and C_j. Blocks $[A_{jk}]$ have the following structure

$$[A_{jk}] = \begin{pmatrix} \mu_{jk} & \eta_{jk} & 0 & \cdots & 0 & \theta_{ij} \\ \eta_{jk} & \mu_{jk} & \eta_{jk} & \cdots & 0 & 0 \\ 0 & \eta_{jk} & \mu_{jk} & \cdots & 0 & 0 \\ \vdots & \vdots & \vdots & \ddots & \vdots & \vdots \\ 0 & 0 & 0 & \cdots & \mu_{jk} & \eta_{jk} \\ \theta_{ij} & 0 & 0 & \cdots & \eta_{jk} & \mu_{jk} \end{pmatrix}_{m\times m,}$$

where $\mu_{jk} = \delta_{jk} + \frac{2}{h^2}a_{jk}$, $\eta_{ij} = -\frac{1}{h^2}a_{jk}$, and

$$\theta_{ij} = \begin{cases} -\frac{1}{h^2}a_{jk} & - \text{ for periodic boundary conditions,} \\ 0 & - \text{ for closed boundary conditions.} \end{cases}$$

The vectors g and c are nm-dimensional, and the matrix $\mathcal{A}$ is $nm \times nm$-dimensional. Moreover matrix $\mathcal{A}$ is sparse with at most $n^2(3m-2)$ (closed boundary conditions) or $3n^2m$ (periodic boundary conditions) nonzero elements. In two-dimensional case (8) we have

$$\begin{aligned} G_j^T &= (g_j(x_1,y_1), g_j(x_1,y_2), \ldots, g_j(x_1,y_m), \\ &\quad g_j(x_2,y_1), g_j(x_2,y_2), \ldots, g_j(x_m,y_m)) \end{aligned}$$

and

$$\begin{aligned} C_j^T &= (c_j(x_1,y_1), c_j(x_1,y_2), \ldots, c_j(x_1,y_m), \\ &\quad c_j(x_2,y_1), c_j(x_2,y_2), \ldots, c_j(x_m,y_m)). \end{aligned}$$

Each of blocks $[A_{jk}]$ is a matrix in the form of

$$[A_{jk}]=\begin{pmatrix} (\alpha_{jk}) & (\beta_{jk}) & (0) & \cdots & (0) & (0) & (\gamma_{jk}) \\ (\beta_{jk}) & (\alpha_{jk}) & (\beta_{jk}) & \cdots & (0) & (0) & (0) \\ (0) & (\beta_{jk}) & (\alpha_{jk}) & \cdots & (0) & (0) & (0) \\ \vdots & \vdots & \vdots & \ddots & \vdots & \vdots & \vdots \\ (0) & (0) & (0) & \cdots & (\alpha_{jk}) & (\beta_{jk}) & (0) \\ (0) & (0) & (0) & \cdots & (\beta_{jk}) & (\alpha_{jk}) & (\beta_{jk}) \\ (\gamma_{jk}) & (0) & (0) & \cdots & (0) & (\beta_{jk}) & (\alpha_{jk}) \end{pmatrix}_{m\times m}$$

consists of smaller blocks, where

$$(\gamma_{ij}) = \begin{cases} (\beta_{jk}) & - \text{ for periodic boundary conditions,} \\ (0) & - \text{ for closed boundary conditions.} \end{cases}$$

Block (0) is $m \times m$-dimensional zero matrix, block (α_{jk}) is in the form of

$$(\alpha_{jk}) = \begin{pmatrix} \mu_{jk} & \eta_{jk} & 0 & \cdots & 0 & \theta_{ij} \\ \eta_{jk} & \mu_{jk} & \eta_{jk} & \cdots & 0 & 0 \\ 0 & \eta_{jk} & \mu_{jk} & \cdots & 0 & 0 \\ \vdots & \vdots & \vdots & \ddots & \vdots & \vdots \\ 0 & 0 & 0 & \cdots & \mu_{jk} & \eta_{jk} \\ \theta_{ij} & 0 & 0 & \cdots & \eta_{jk} & \mu_{jk} \end{pmatrix}_{m\times m,}$$

where $\mu_{jk} = \delta_{jk} + \frac{4}{h^2}a_{jk}$, $\eta_{ij} = -\frac{1}{h^2}a_{jk}$ and

$$\theta_{ij} = \begin{cases} -\frac{1}{h^2}a_{jk} & - \text{ for periodic boundary conditions,} \\ 0 & - \text{ for closed boundary conditions,} \end{cases}$$

Block (β_{jk}) is in the form of diagonal

$$(\beta_{jk})=\begin{pmatrix} \frac{-1}{h^2}a_{jk} & 0 & 0 & \cdots & 0 & 0 & 0 \\ 0 & \frac{-1}{h^2}a_{jk} & 0 & \cdots & 0 & 0 & 0 \\ 0 & 0 & \frac{-1}{h^2}a_{jk} & \cdots & 0 & 0 & 0 \\ \vdots & \vdots & \vdots & \ddots & \vdots & \vdots & \vdots \\ 0 & 0 & 0 & \cdots & \frac{-1}{h^2}a_{jk} & 0 & 0 \\ 0 & 0 & 0 & \cdots & 0 & \frac{-1}{h^2}a_{jk} & 0 \\ 0 & 0 & 0 & \cdots & 0 & 0 & \frac{-1}{h^2}a_{jk} \end{pmatrix}_{m\times m.}$$

The vectors g and c are nm^2-dimensional, and the matrix $\mathcal{A}$ is $nm^2 \times nm^2$-dimensional. As in the previous case, matrix $\mathcal{A}$ is sparse. It has at most $n^2(5m-4)m$ (closed boundary conditions) or $5n^2m^2$ (periodic boundary conditions) nonzero elements. As basis functions $\{\phi_j : j = 1, 2, ..., \infty\}$ one can choose any polynomials orthogonal with respect to some weight function W.

In our numerical scheme we use Legendre polynomials, which are orthogonal on the interval $[-1, 1]$ with respect to weight function $W \equiv 1$. We obtain orthonormality on the interval $[0, t]$ by scaling argument of the function and using normalisation factor, i.e.

$$\phi_j(x) = \sqrt{\frac{2k-1}{t}}P_{k-1}\left(\frac{2x}{t}-1\right), \tag{11}$$

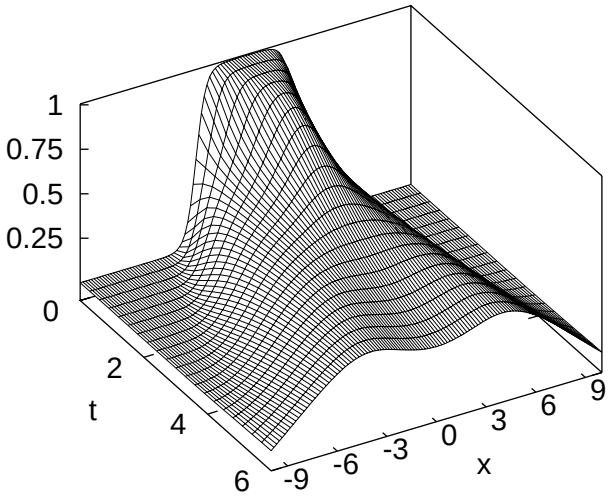

Fig. 1. Numerical solutions to Volterra equation (1) in 1 spatial dimension: $\alpha = 1.5$, $t \in [0, 6]$, closed boundary conditions.

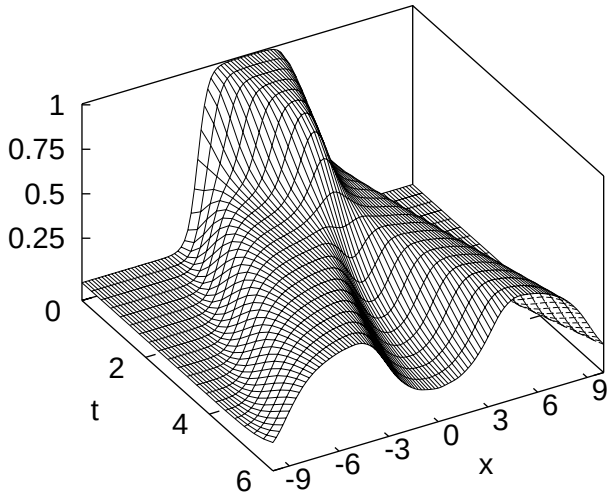

Fig. 2. Numerical solutions to Volterra equation (1) in 1 spatial dimension: $\alpha = 1.85$, $t \in [0, 6]$, closed boundary conditions.

where $\{P_k : k = 0, 1, 2, ..., \infty\}$ are Legendre polynomials.

The matrix $\mathcal{A}$ of the linear system (9) is sparse, what in conjunction with large matrix size suggests use of iterative methods for solving linear systems. Morover, the matrix $\mathcal{A}$ is nonsymmetric. Our numerical results were obtained with two different iterative methods. First one, GMRES (Generalized minimal resiudal method) (Saad and Schultz, 1986), approximates the solution by the vector with minimal residual in a Krylov subspace found with use of Arnoldi iteration. Second one, Bi-CGSTAB (BiConjugate Gradient Stabilized method) (Van der Vorst, 1992), was developed to solve non-symmetric linear systems. It avoids irregular convergence patterns of CGS (Conjugate Gradient Squared method) (Barrett *et al.*, 1994). In both methods a suitable preconditioning is necessary. For our purposes GMRES appeared more efficient. It was converging faster and usually required less iterations than Bi-CGSTAB method.

For three spatial dimensions vectors g and c in (9) become nm^3-dimensional. The matrix $\mathcal{A}$ preserves its block nested structure (10) but with one more level of nesting. The number of the nonzero elements of matrix $\mathcal{A}$ reaches the order of $7n^2m^3$. Therefore, the numerical solution for $d = 3$ case require much more computer power than for one and two-dimensional cases.

3. Examples of numerical results

Analytical solutions to the fractional equations are of great importance but they are hardly computable. In most cases to obtain a solution to a particular problem one has to apply a suitable numerical methods. In (Rozmej and Karczewska, 2005) we have shown that for the cases when analytical solutions are known in terms of elementary functions (1+1-dimensional cases with $\alpha = 1$ and $\alpha = 2$) our approximate numerical solution reproduces the analytical ones with high accuracy.

We present numerical results to Volterra equation (1) in three cases. In one spatial dimension with closed boundary conditions (Fig. 1 and 2) and in two spatial dimensions with both closed (Fig. 3 and 4) and periodic boundary conditions (Fig. 5 and 6).

For presentation of the results we have chosen as initial conditions the Fermi distribution:

$$u(\vec{r}, 0) = \frac{1}{1 + \exp \frac{r - r_0}{a}} \tag{12}$$

where $r = \sqrt{\sum_{i=1}^{d} x_i^2}$ and d is the space dimension. The constants in (12) are taken as: $r_0 = 3$, $a = 0.3$.

In Table 1 parameters m (number of grid points in space variables) and n (number of basis functions) used to obtain numerical results are presented. In principle, when the basis of orthonormal functions is richer then the

Table 1. Parameters

Case	Grid size	Basis functions
d=1	121	21
d=2, closed b. c.	101×101	21
d=2, periodic b. c.	71×71	21

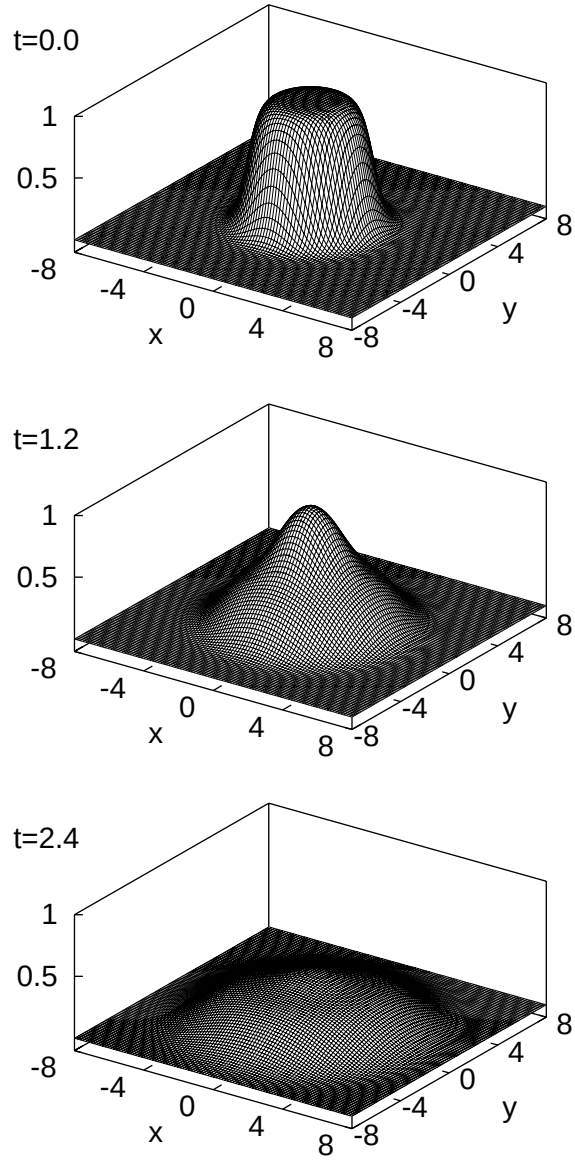

Fig. 3. Numerical solutions to Volterra equation (1) in 2 spatial dimensions at chosen time steps: $\alpha = 1.5$, closed boundary conditions.

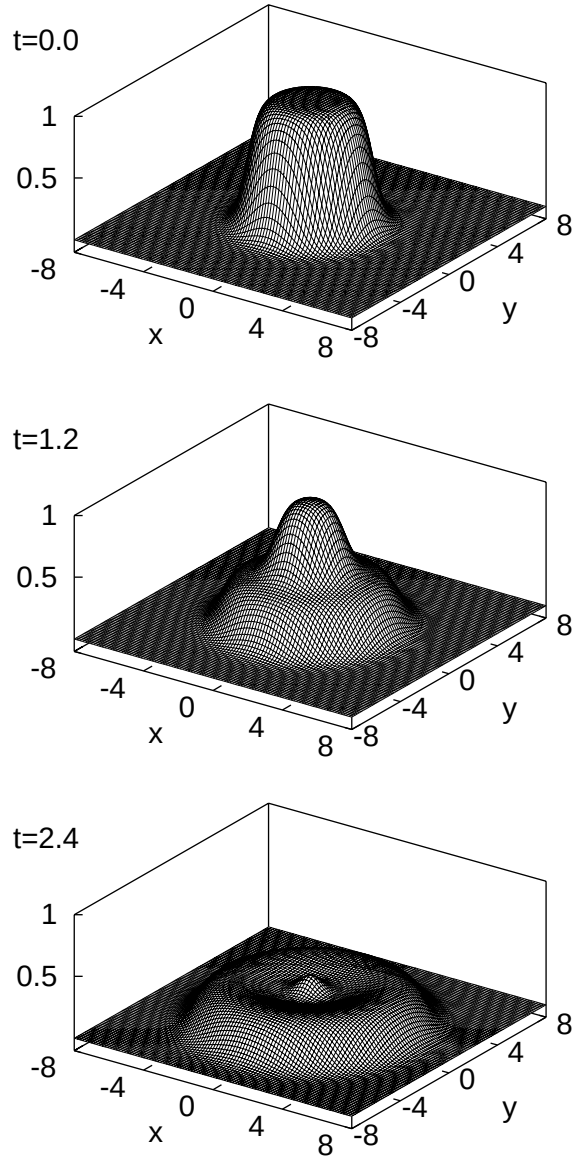

Fig. 4. Numerical solutions to Volterra equation (1) in 2 spatial dimensions at chosen time steps: $\alpha = 1.85$, closed boundary conditions.

numerical results are more precise. The similar argument applies to the number of grid points taken in the discretization of the problem. However, the growing size of matrices (as the result of increase of the number of grid points and basis functions) results in an incrementation of the number of computer operations and in the accumulation of round-off errors.

Comparing Figs. 3 and 4 or Figs. 5 and 6 one can notice that for 1+2-dimensional case the increase of α changes the time evolution from diffussion-like behavior to wave-like one. Comparison of the results obtained with the same α (for instance Figs. 3 and 5 or Figs. 4 and 6) show the influence of 'waves' incoming to the given space cell from the neighbours.

The method used in the paper has some limitations. Numerical approximation of the second derivatives (Laplacian) can be good enough when the initial condition $u(x, 0)$ is relatively smooth function, *i.e.* varies not rapidly with respect to space variables within a range of grid points.

Figs. 1 and 2 shows the time evolution for fractional time derivative of the order $\alpha = 1.5$ and $\alpha = 1.85$, re-

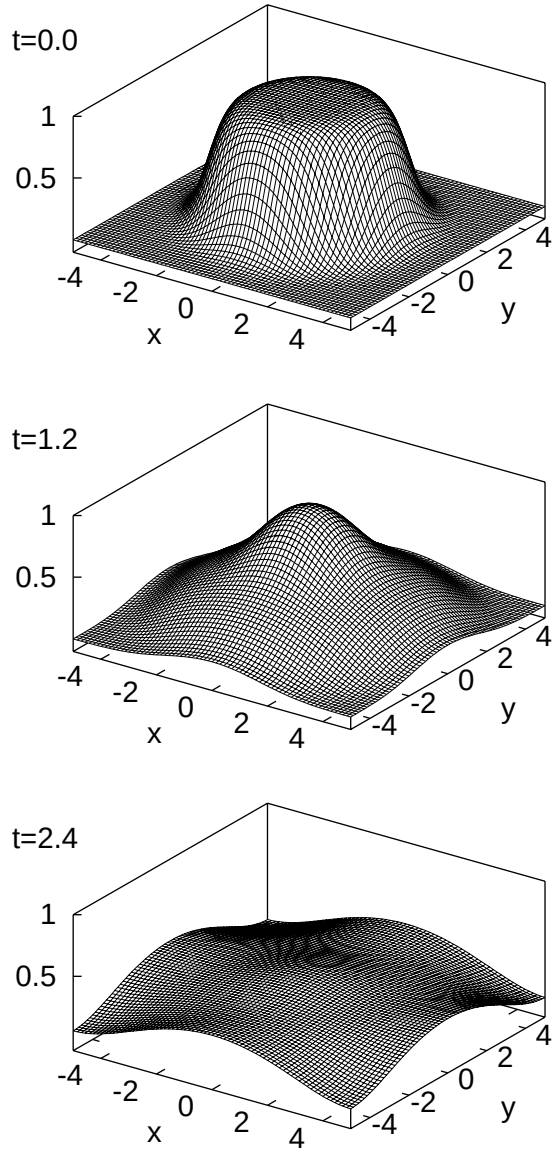

Fig. 5. Numerical solutions to Volterra equation (1) in 2 spatial dimensions at chosen time steps: $\alpha = 1.5$, periodic boundary conditions.

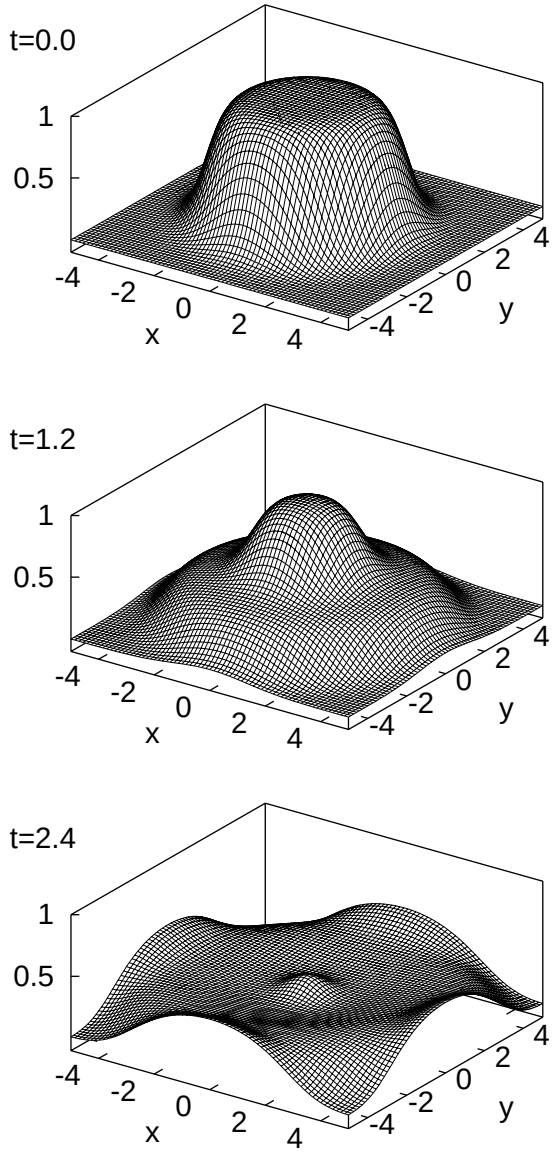

Fig. 6. Numerical solutions to Volterra equation (1) in 2 spatial dimensions at chosen time steps: $\alpha = 1.85$, periodic boundary conditions.

spectively. One can clearly see that the system evolves in a way which exhibits wave motion with a diffusive character. When α varies towards 1 one obtains more diffusion-like evolution, whereas for α closer to 2 the wave-like evolution becomes dominant. The closed (or free) boundary conditions mean that the initial system can in principle evolve to infinity in space variable, where initially the value of $u(x, 0) = 0$. In the presented figures, however, the solution is cut of to the range of the space variable where the solutions differs from zero substantially.

4. Approximation errors

As mentioned earlier the analytic form of the solution $u(x, t)$ is known only for one space dimension (Fujita, 1990; Schneider and Wyss, 1989). However, the analytical solutions for cases different than $\alpha = 1$ and $\alpha = 2$, given in terms of Mittag-Leffler functions are practically non-computable. To estimate the quality of the numerical solutions several tests have been performed. For $d = 1$ and $\alpha = 1$ and $\alpha = 1$ we can compare the analytical solution with the numerical one obtained from (3) and (9). We define, as an error estimate, the maximum of the ab-

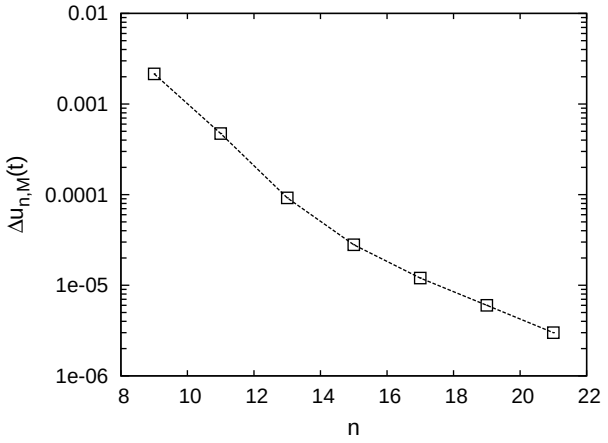

Fig. 7. The error estimate (13), $\Delta u_{n,M}(t)$ - the maximum difference between approximate solutions for which the number of basis functions differs by 2 as function of n for one spatial dimension $d = 1$. Case $m = 121$, $\alpha = 1.5$ and $t = 1.8$ is displayed.

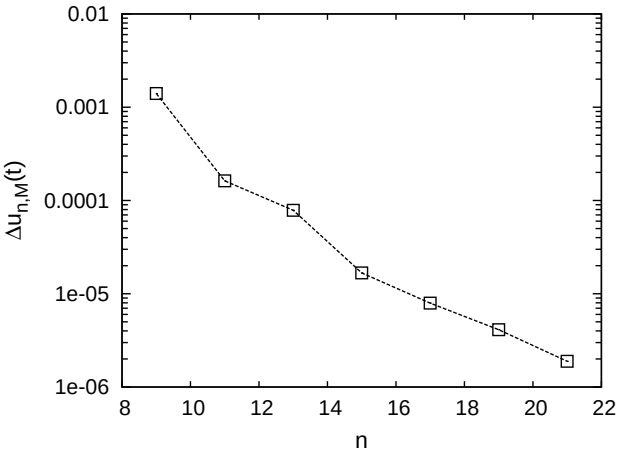

Fig. 8. The same as in Figure 7 but for two spatial dimensions $d = 2$ and grid size $m = 101$.

solute value of the difference between the exact analytical solution and approximate numerical one

$$\Delta u_{n,m}(t) = \max \left| u^{\mathrm{anal}}_{n,m}(x_i,t) - u^{\mathrm{num}}_{n,m}(x_i,t) \right|^{m}_{i=1} ,$$

where maximum is taken over all grid points x_i. For $d = 1$ and $\alpha = 1$ and 2, $n > 20$, $m > 100$, $t \leq 6$ the error estimate $\Delta u_{n,m}(t)$ was always less than $10^{-5} - 10^{-6}$.

For cases when we have to relay only on the approximate numerical solutions ($1 < \alpha < 2$) we procede in a different way. One can expect that when the number of basis functions (n in (3)) or the size of grid (m) increases a better approximation of the solution is obtained. In order to show that trend we define the absolute value of the difference between the two approximate solutions taken for different basis subspaces and the same grid size

$$\Delta u_{n,M}(t) = \max \left| u^{\mathrm{num}}_{n,M}(x_i,t) - u^{\mathrm{num}}_{n-2,M}(x_i,t) \right|^{M}_{i=1} , \quad (13)$$

where $M = m^d$. In Fig. 7 the error estimate $\Delta u_{n,M}(t)$ is presented for one-dimensional case ($d = 1$), $\alpha = 1.5$, grid size $m = 121$ and $t = 1.8$ in a semilogarithmic plot. The two-dimensional case ($d = 2$), $m = 101$ and the same values of α and t is displayed in Fig. 8. In the both Figs 7 and 8 the error estimates exhibit almost exponential decrease with the growth of basis subspace n (3).

Comparing the approximate solutions for different grid sizes is a little more difficult because their values are given at different points. Therefore, in order to compare them we define the error estimate in the following way:

$$\Delta u_{n,m}(t) = \max \left| u^{\mathrm{num}}_{n,m}(x_i,t) - \tilde{u}^{\mathrm{num}}_{n,m'}(x_i,t) \right|^{M}_{i=1} . \quad (14)$$

In (14), $\tilde{u}^{\mathrm{num}}_{n,m'}(x_i,t)$ stands for the value in point of the bigger grid m obtained from the solution on smaller grid m' by cubic spline interpolation. Fig. 9 shows an example of the decrease of the error estimate $\Delta u_{n,m}(t)$ for $d = 2$ dimension. For the one-dimensional calculations (not shown here) the results exhibit the same behaviour. We see that for the fixed basis subspace the increase of the grid size leads to substantial decrease of the error estimate. That decrease is, for larger values of m, close to exponential decrease.

That almost exponential decrease of the error estimate as the function of the number of the basis functions (with fixed grid) or as the the function of the grid size (with fixed basis) suggest that in principle one can obtain the numerical solution with arbitrary precision chos-

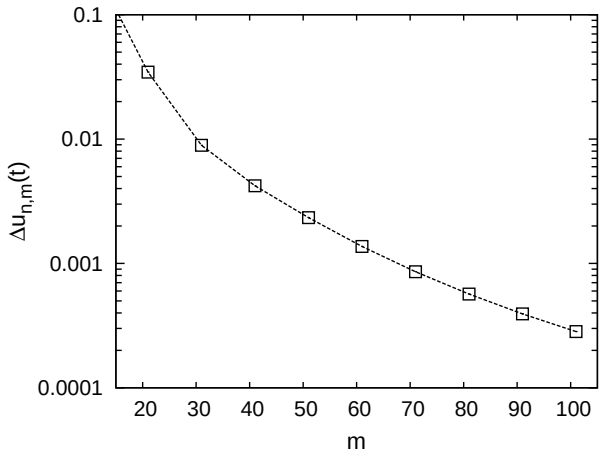

Fig. 9. The error estimate (14), $\Delta u_{n,m}(t)$ - the maximum difference between consecutive results obtained for grid sizes m and $m' = m - 10$ in 2 spatial dimensions. The case $n = 21$ basis functions, $\alpha = 1.5$ and $t = 1.8$ is presented.

ing appropriate basis and grid sizes. However, the bigger the basis and the grid size are, the larger number of the computer operations is necessary to obtain the solution. To avoid the accumulation of round-off errors with the increase of computer operations one needs to apply higher and higher precision (longer computer word) what results in much longer execution time and demands much more computer power. In practice, the reasonable compromise between the precision and computational effort is chosen for a given problem.

The results for 3-dimensional case show the similar qualitative behaviour. We do not present them here because the computing time grows substantialy. The case $d = 3$ and $m = 21$ requires the same order of computer operations as the case $d = 2$, $m = 101$ with the same n. The test computations made for grid sizes up to $m = 21$ and the number of basis functions up to $n = 20$ gave trends which qualitatively agree with those for $d = 2$.

5. Conclusions

We presented a succesful numerical method of solving a class of Volterra equations (1) which are equivalent to differential equations with fractional time (2). From our results the following conclusions can be drawn:

- For spatially smooth enough initial conditions and reasonable choice of the (n, m) parameters the errors of the approximate numerical solution may be kept on a desired level.

- Our method works well for $d = 1$ and $d = 2$ spatial dimensions. However, the larger d is, the more computer power is necessary. Test calculations indicate that the metod should work for $d = 3$, too.

References

Barrett, R., Berry, M., Chan, T. F., Demmel, J., Donato, J., Dongarra, J., Eijkhout, V., Pozo, R., Romine, C. and der Vorst, H. V. (1994). *Templates for the Solution of Linear Systems: Building Blocks for Iterative Methods, 2nd Edition*, SIAM, Philadelphia, PA.

Bazhlekova, E. (2001). *Fractional Evolution Equations in Banach Space*, Ph.D. Dissertation, Eindhoven University of Technology.

Ciesielski, M. and Leszczyński, J. (2006). Numerical treatment of an initial-boundary value problem for fractional partial differential equations, *Signal Processing* **86**: 2619–2631.

Fujita, Y. (1990). Integrodifferential equation which interpolates the heat equation and the wave equation, *Osaka Journal of Mathematics* **27**(2): 309–321.

Gambin, Y., Massiera, G., Ramos, L., Ligoure, C. and Urbach, W. (2005). Bounded step superdiffusion in an oriented hexagonal phase, *Physical Review Letters* **94**: 110602.

Goychuk, I., Heinsalu, E., Patriarca, M., Schmid, G. and Hänggi, P. (2006). Current and universal scaling in anomalous transport, *Physical Review E* **73**: 020101‘(R)’.

Guermah, S., Djennoune, S. and Betteyeb, M. (2008). Controllability and observability of linear discrete-time fractional-order systems, *International Journal of Applied Mathematics and Computer Science* **18**(2): 213–222.

Heinsalu, E., Patriarca, M., Goychuk, I. and Hänggi, P. (2009). Fractional Fokker-Planck subdiffusion in alternating fields, *Physical Review E* **79**: 041137.

Heinsalu, E., Patriarca, M., Goychuk, I., Schmid, G. and Hänggi, P. (2006). Fokker-Planck dynamics: Numerical algorithm and simulations, *Physical Review E* **73**: 046133.

Kaczorek, T. (2008). Fractional positive continuous-time linear systems and their reachability, *International Journal of Applied Mathematics and Computer Science* **18**(2): 223–228.

Kou, S. and Sunney Xie, X. (2004). Generalized Langevin equation with fractional gaussian noise: subdiffusion within a single protein molecule, *Physical Review Letters* **93**: 180603.

Labeyrie, G., Vaujour, E., Müller, C., Delande, D., Miniatura, C., Wilkowski, D. and Kaiser, R. (2003). Slow diffusion of light in a cold atomic cloud, *Physical Review Letters* **91**: 223904.

Meltzer, R. and Klafter, J. (2000). The random walk’s guide to anomalous diffusion: a fractional dynamics approach, *Physics Reports* **339**(1): 1–77.

Ratynskaia, S., Rypdal, K., Knapek, C., Kharpak, S., Milovanov, A., Ivlev, A., Rasmussen, J. and Morfill, G. (2006). Superdiffusion and viscoelastic vortex flows in a two-dimensional complex plasma, *Physical Review Letters* **96**: 105010.

Rozmej, P. and Karczewska, A. (2005). Numerical solutions to integrodifferential equations which interpolate heat and wave equations, *International Journal on Differential Equations and Applications* **10**(1): 15–27.

Saad, Y. and Schultz, M. (1986). GMRES: A Generalized Minimal Residual algorithm for solving nonsymmetric linear systems, *SIAM Journal on Scientific and Statistical Computing* **7**(3): 856–869.

Schneider, W. and Wyss, W. (1989). Fractional diffusion and wave equations, *Journal of Mathematical Physics* **30**: 134–144.

Van der Vorst, H. (1992). Bi-CGSTAB: A fast and smoothly converging variant of Bi-CG for the solution of non-symmetric linear systems, *SIAM Journal on Scientific and Statistical Computing* **13**(2): 631–644.